www.nature.com/aps

Acta Pharmacologica Sinica

ARTICLE

β-arrestin2 deficiency ameliorates S-100-induced autoimmune hepatitis in mice by inhibiting infiltration of monocyte-derived macrophage and attenuating hepatocyte apoptosis

Ting-ting Chen[1], Xiu-qin Li[1], Nan Li[1], Ya-ping Xu[1], Yu-han Wang[1], Zi-ying Wang[1], Sheng-nan Zhang[1], Meng Qi[1], Shi-hao Zhang[1], Wei Wei[1]✉, Hua Wang[2]✉ and Wu-yi Sun[1]✉

Autoimmune hepatitis (AIH) is a progressive hepatitis syndrome characterized by high transaminase levels, interface hepatitis, hypergammaglobulinemia, and the presence of autoantibodies. Misdiagnosis or delayed treatment of AIH can lead to cirrhosis or liver failure, which poses a major risk to human health. β-Arrestin2, a key scaffold protein for intracellular signaling pathways, has been found to be involved in many autoimmune diseases such as Sjogren's syndrome and rheumatoid arthritis. However, whether β-arrestin2 plays a role in AIH remains unknown. In the present study, S-100-induced AIH was established in both wild-type mice and β-arrestin2 knockout (*Arrb2* KO) mice, and the experiments identified that liver β-arrestin2 expression was gradually increased, and positively correlated to serum ANA, ALT and AST levels during AIH progression. Furthermore, β-arrestin2 deficiency ameliorated hepatic pathological damage, decreased serum autoantibody and inflammatory cytokine levels. β-arrestin2 deficiency also inhibited hepatocyte apoptosis and prevented the infiltration of monocyte-derived macrophages into the damaged liver. In vitro experiments revealed that β-arrestin2 knockdown suppressed the migration and differentiation of THP-1 cells, whereas β-arrestin2 overexpression promoted the migration of THP-1 cells, which was regulated by the activation of the ERK and p38 MAPK pathways. In addition, β-arrestin2 deficiency attenuated TNF-α-induced primary hepatocyte apoptosis by activating the Akt/GSK-3β pathway. These results suggest that β-arrestin2 deficiency ameliorates AIH by inhibiting the migration and differentiation of monocytes, decreasing the infiltration of monocyte-derived macrophages into the liver, thereby reducing inflammatory cytokines-induced hepatocytes apoptosis. Therefore, β-arrestin2 may act as an effective therapeutic target for AIH.

Keywords: autoimmune hepatitis; β-arrestin2; monocyte; macrophage; hepatocyte; MCP-1; TNF-α

Acta Pharmacologica Sinica (2023) 44:2048–2064; https://doi.org/10.1038/s41401-023-01103-9

INTRODUCTION

Autoimmune hepatitis (AIH) is a parenchymal inflammation of the liver characterized by the infiltration of inflammatory cells into the portal area, hepatocyte damage, hypergammaglobulinemia, as well as positive autoantibodies [1]. Globally, AIH occurs in all ages and ethnicities, with a recent increase in incidence and prevalence worldwide. Approximately 40% of patients with AIH can develop fibrosis or cirrhosis, which are risk factors for the development of hepatocellular carcinoma [2]. Since the etiology of AIH remains unelucidated, it is crucial to study the pathogenesis of AIH and explore its possible therapeutic targets.

At present, no effective cure for AIH is available, and treatment goal is to prevent disease progression by ameliorating inflammatory responses. Immune cell migration to the damaged liver appears to be the initial key process in liver inflammation, mediating a series of inflammatory responses that ultimately leads to continuous immune cell recruitment, hepatocyte apoptosis, and tissue damage [3]. Increasing evidence suggests the vital role of monocyte-derived macrophages in liver inflammation and the abundance of activated macrophages in the portal veins and interface hepatitis sites in patients with AIH [4, 5]. When AIH occurs, liver-resident cells secrete monocyte chemoattractant protein 1 (MCP-1), triggering the infiltration of a large number of monocyte-derived macrophages into the damaged liver. Accumulated and activated macrophages can directly or indirectly aggravate the inflammatory responses of the liver and result in hepatocyte necrosis and apoptosis, damaging the tissue structure, which further induces liver dysfunction [6, 7]. Moreover, previous studies have reported that an imbalance in the apoptotic pathways is a key element involved in the pathogenesis and severity of AIH and that the abnormal signals in these pathways may act as feasible therapeutic targets [8, 9]. These findings suggest that the targeted regulation of monocyte-derived macrophage infiltration and hepatocyte apoptosis contribute to AIH treatment.

β-arrestin2 was originally identified as a regulatory protein of the G-protein-coupled receptor signaling pathway [10]. However, recent studies have reported the role of β-arrestin2 as an

[1]Institute of Clinical Pharmacology, Anhui Medical University, Key Laboratory of Anti-inflammatory and Immune Medicine, Ministry of Education, Anhui Collaborative Innovation Center of Anti-inflammatory and Immune Medicine, Hefei 230032, China and [2]Department of Oncology, the First Affiliated Hospital of Anhui Medical University, Hefei 230022, China
Correspondence: Wei Wei (wwei@ahmu.edu.cn) or Hua Wang (wanghua@ahmu.edu.cn) or Wu-yi Sun (sunwuyi51@aliyun.com)
These authors contributed equally: Ting-ting Chen, Xiu-qin Li

Received: 1 November 2022 Accepted: 1 May 2023
Published online: 25 May 2023

important scaffold protein that can modulate several signaling pathways, including the tyrosine kinase and mitogen-activated protein kinase (MAPK) pathways, to mediate various cellular biological responses, including cell migration, differentiation, proliferation and apoptosis [11]. Moreover, previous studies reported that β-arrestin2 expression was abnormally elevated in mouse liver during liver fibrosis and acute liver injury (ALI) and that β-arrestin2 deficiency can ameliorate liver fibrosis by suppressing collagen deposition and reactive oxygen species (ROS) production in hepatic stellate cells as well as improve ALI by decreasing ROS production [12–14]. However, the role of β-arrestin2 in AIH remains unelucidated.

As a result, the present study aimed to identify the involvement of β-arrestin2 in AIH pathogenesis. We developed an S-100-induced AIH mice model and found that liver β-arrestin2 expression was increased during AIH progression. Furthermore, we found that β-arrestin2 deficiency alleviates inflammatory cell infiltration and hepatocyte apoptosis in AIH. Moreover, in vitro experiments indicated that β-arrestin2 deficiency exerts a protective effect against S-100-induced AIH by inhibiting the infiltration of monocyte-derived macrophages by inhibiting the extracellular signal-regulated kinase (ERK) and p38 MAPK signaling pathways and attenuating hepatocyte apoptosis by activating Akt/glycogen synthase kinase 3 beta (GSK-3β) signaling pathway. The results of our study suggest the role of β-arrestin2 as a therapeutic target for AIH.

MATERIALS AND METHODS

Animals

Wild-type (WT) C57BL/6 J mice were purchased from the Animal Center of Anhui Medical University. β-arrestin2 knockout (*Arrb2* KO) C57BL/6 J mice were provided by Jackson Laboratory (Maine, USA). Each mouse was genotyped and identified at 21 days after birth as previously described, and age- and sex-matched littermates were selected for the experiments [15]. All animals are housed in a specific-pathogen-free environment with a temperature of 25 °C ± 2 °C and relative humidity of 55% ± 10%. The mice were provided *ad libitum* access to food and water throughout the experiment. The Animal Experiment Ethics Review Committee of the Institute of Clinical Pharmacology, Anhui Medical University approved all animal experiments. The experiments were performed strictly according to the guidelines of the Animal Care and Use Committee of Anhui Medical University.

Animal model of AIH

The liver was perfused with phosphate-buffered saline (PBS) to obtain fresh hepatic antigen S-100 using a previously described method [16]. The immune agent was prepared by emulsifying S-100 with an equal volume of Freund's complete adjuvant (Sigma, MO, USA). The *Arrb2* KO and WT mice were divided into normal and model mice, respectively. The mice in the model group were first immunized by intraperitoneally injecting 0.5 mL of the immune agent. After 7 days, a second immunization was performed using the same method to establish the AIH mice model. The mice in the control group were intraperitoneally injected with 0.9% saline solution. All experimental mice were sacrificed 28 days after initiating modeling.

Histopathological analysis

Liver tissues were embedded in paraffin for preparing 5 μm-thick sections. Then, to observe the pathological changes in the tissue, hematoxylin and eosin (H&E) staining was performed. The liver sections were first stained with hematoxylin and then with eosin. Finally, the slides were routinely visualized for morphological changes under the Olympus BX53 light microscope (Olympus Corporation, Tokyo, Japan).

Measurement of serum aminotransferase activities and autoantibody levels

Serum alanine aminotransferase (ALT) and aspartate aminotransferase (AST) activities were measured using the Hitachi 3100 Automatic Analyzer (Hitachi, Japan) according to the manufacturer's instructions. Serum antinuclear antibody (ANA) levels were measured using commercial mouse Enzyme-Linked Immunosorbent Assay (ELISA) kits (Enzyme-linked Biotechnology Co. Ltd., Shanghai, China) according to the manufacturer's instructions.

Isolation of hepatocytes

A two-step collagenase digestion and gradient centrifugation approach was used to isolate mouse primary hepatocytes and hepatic nonparenchymal cells, as previously described [17]. Mice were anesthetized and the peritoneal cavity was opened. First, the inferior vena cava was intubated and cutted off. Next, the liver was perfused with in D-Hank's buffer containing 0.5 mmol/L ethylenediaminetetraacetic acid at 37 °C. The liver was subsequently removed, placed in a sterile dish, and supplemented with 0.05% collagen IV (Sigma) digestion buffer. Then, the liver was cut into pieces and shaken at 200 r/min for 30 min in an incubator at 37 °C. Finally, Dulbecco's modified Eagle's medium with 1% penicillin–streptomycin solution (Beyotime Biotechnology, Shanghai, China) and 10% fetal bovine serum (FBS) (WISENT INC, Canada) was added and primary hepatocytes were harvested by centrifuging the samples at 400 r/min for 5 min.

Flow cytometric analysis

First, mice were anesthetized and sacrificed; then, the spleen tissue was isolated, single-cell spleen suspension was harvested, and splenic lymphocytes were isolated from the gradient interface. The collected hepatic nonparenchymal cells and splenic lymphocytes were incubated with fluorescently labeled anti-mouse antibodies in PBS containing 2% FBS for 30 min in the dark. The following antibodies were used for flow cytometry: anti-CD3-PE, anti-CD4-FITC, anti-CD25-APC (BD Pharmingen, CA, USA), anti-CD8-APC, anti-IFN-γ-APC, anti-IL-4-PE (BioLegend, CA, USA), anti-IL-17-PE-cy7, and anti-Foxp3-PE (Invitrogen, CA, USA). For detecting macrophage infiltration in AIH, we incubated the isolated hepatic nonparenchymal cells with the following fluorescently labeled anti-mouse antibodies for 30 min in the dark: anti-CD45-PE, anti-CD11b-BV421, anti-F4/80-APC (BioLegend), and anti-Ly6C-FITC (Miltenyi Biotec, BG, Germany).

The differentiation of THP-1 cells, a human leukemia monocytic cell line, was detected and characterized using flow cytometry. The cells were treated with phorbol-12-myristate-13-acetate (PMA), harvested, and incubated with anti-human CD68-BV421 and anti-human CD36-PE-cy5.5 antibodies (BioLegend) for 30 min. All fluorescence-activated cell sorting data were collected and analyzed using the CytoFLEX flow cytometer (Beckman Coulter, Inc., CA, USA).

Immunofluorescence staining

Frozen liver sections were fixed and blocked. To study active caspase-3 activity in the mouse liver, the sections were incubated overnight with the anti-caspase-3 antibody (1:100) (Bioss, Beijing, China). Thereafter, the sections were treated for 1 h in the dark with anti-rabbit Alexa Fluor 555 conjugated antibodies (Thermo Fisher, MA, USA). To detect tumor necrosis factor α (TNF-α) secretion by macrophages in AIH, we performed the immunofluorescence double-labeling assay to detect TNF-α and F4/80 expression in the liver tissues. The sections were incubated overnight with anti-F4/80 antibody (1:100) (Abcam, MA, USA) and anti-TNF-α antibody (1:100) (Cell Signaling, MA, USA) and then treated with anti-rabbit Alexa Fluor 555 conjugated antibodies and anti-mouse Alexa Fluor 488 conjugated antibodies for 1 h in the dark. The cell nuclei were finally labeled with 4′,6-diamidino-2-phenylindole (DAPI).

THP-1 cells have been widely used to study the biology and function of human monocytes and macrophages; PMA can induce the differentiation of THP-1 cells into macrophages [18]. We used PMA (Sigma) to induce THP-1 cell differentiation for 48 h. Cells were incubated overnight with rabbit anti-CD68 antibody (diluted 1:100) (Affinity, USA) and then with anti-rabbit Alexa Fluor 555-conjugated antibody for 1 h. DAPI was used to label the cell nuclei. All fluorescence results were obtained using the Leica TCS SP8 confocal laser scanning microscope (Leica Biosystems, Wetzlar, Germany).

Terminal deoxynucleotidyl transferase biotin-dUTP nick end labeling (TUNEL) assay for apoptosis detection

To detect the apoptosis of hepatocytes in mice with AIH, frozen liver sections were harvested for the TUNEL assay. DNA fragmentation in the cell nucleosome was detected using the TUNEL assay with the in situ apoptosis detection kit (Vazyme, Nanjing, China) according to the manufacturer's instructions. TUNEL-positive cells (green) were observed under the Leica TCS SP8 confocal laser scanning microscope (Leica Biosystems).

Cell culture and treatment

THP-1 cells (Procell Life Science &Technology Co, Ltd, Wuhan, China) were cultured in RPMI-1640 medium (Gibco, Thermo Fisher, CA, USA) supplemented with 1% penicillin–streptomycin solution and 10% FBS. These cells were treated with 10 ng/mL MCP-1 (Peprotech, NJ, USA) or 100 ng/mL PMA (Sigma), followed by subsequent experiments for evaluating monocyte migration and differentiation, respectively.

siRNA and overexpression plasmid transfection

β-arrestin2 expression was knocked down via siRNA transfection. THP-1 cells were transfected with a specific siRNA targeting β-arrestin2 (GenePharma, Shanghai, China) for 6 h in 6-well plates using Lipofectamine® RNAiMAX (Invitrogen); scrambled RNA was used as a negative control. For the β-arrestin2 overexpression experiment, the pcDNA/β-arrestin2 overexpression plasmid was used. The β-arrestin2 overexpression plasmid was transfected into THP-1 cells in 6-well plates using the jetOPTIMUS DNA Transfection Reagent (Polyplus-transfection, Illkirch, France). The transfection efficiency of the siRNA and overexpression plasmid was analyzed using Western blotting. In addition, the β-arrestin2 overexpression plasmid was transfected into THP-1 cells in the presence or absence of 50 μmol/L SB203580 (a p38 MAPK inhibitor) or PD98059 (an ERK1/2 inhibitor) (MedChemExpress, NJ, USA).

Transwell assay for cell migration

An 8-μm pore size Transwell insert plate (Corning, USA) was used for the migration assay, which was performed in 24-well plates. In the upper chamber, untreated THP-1 cells (1×10^5/mL) with 100 μL of serum-free medium were seeded. In the lower chamber, 600 μL of medium containing 10% FBS and 10 ng/mL MCP-1 was added. The cells were cultured for 2 h, followed by the removal of the chamber. Nonmigrated cells present above the filter were removed using a cotton swab. After fixing the cells, the migrated cells under the chamber were stained with 0.1% crystal violet (Beyotime Biotechnology). The Olympus BX53 microscope (Olympus Optical Co. Ltd.) was used for cell counting in five random fields per well.

Filamentous actin (F-actin) staining

F-actin was stained with TRITC–phalloidin (Dalian Meilun Biotechnology Co., Ltd. Dalian, China). β-arrestin2-silenced or -overexpressing THP-1 cells were treated with MCP-1 for 2 h. Then, the cells were fixed with 4% paraformaldehyde, followed by the addition of 0.1% Triton X-100 to permeate the cells. Finally, the cells were stained with TRITC–phalloidin solution (TRITC–phalloidin: PBS = 1:1000, containing 1% bovine serum albumin) for 40 min in the dark. DAPI was used for cell nuclei counterstaining. Images were visualized under a confocal laser scanning microscope.

Preparation of the conditioned media (CM) for THP-1-derived macrophages

PMA-induced THP-1 cells were differentiated into macrophages. Then, the following CM of THP-1-derived macrophages were collected for future use: THP-1-derived macrophages without any treatment; THP-1-derived macrophages treated with 100 ng/mL lipopolysaccharide (LPS) (Sigma) for 4 h; and THP-1-derived macrophages transfected with β-arrestin2 siRNA or overexpression plasmid, followed by LPS stimulation. After performing the aforementioned treatments, the medium in each group was replaced with serum-free fresh medium, followed by incubation for 2 days before collecting the CM. Cell debris from the supernatants was removed via centrifugation before using in subsequent experiments.

Detection of inflammatory cytokine levels

TNF-α, IL-1β, and interleukin-6 (IL-6) levels were measured in the serum and liver homogenates of AIH mice using mouse ELISA kits according to standardized techniques. The levels of TNF-α in the CM of THP-1-derived macrophages were also evaluated using human ELISA kits (Enzyme-linked Biotechnology Co. Ltd.). The absorbance was measured at a wavelength of 450 nm using the BioTek Elx × 808 microplate reader (BioTek, Winooski, VT, USA). Finally, the standard curve was prepared to calculate sample concentrations.

Flow cytometric analysis for hepatocyte apoptosis

To elucidate the effect of TNF-α from macrophages on hepatocyte apoptosis, the L02 human liver cell line (Cell Bank of Chinese Academy of Sciences, Shanghai, China) was cultured with the CM for 24 h to observe apoptosis. Additionally, isolated primary hepatocytes were treated with TNF-α (Peprotech) for 24 h and collected. The apoptosis of L02 cells and primary hepatocytes were quantified using the FITC–Annexin V Apoptosis Detection Kit (BestBio, Shanghai, China) according to the manufacturer's instructions. The cells were resuspended in annexin binding buffer and treated with 5 μL of FITC–annexin V for 15 min and then stained with 6 μL of propidium iodide solution for 5 min. The cell apoptosis rates were recorded using the CytoFLEX flow cytometer.

Western blot analysis

Total protein was extracted from liver tissues and THP-1 cells using a previously described method [14]. Sodium dodecyl sulfate–polyacrylamide gel electrophoresis was performed to separate the target protein, followed by transferring the gel onto a polyvinylidene fluoride membrane (Millipore, Bedford, MA). The membranes were placed in 0.05% Tween 20–PBS containing 5% skimmed milk for 2 h and then incubated overnight with the primary antibody. The primary antibodies used were as follows: anti-β-actin, anti-β-arrestin2, anti-MCP-1 (Affinity, USA), anti-ERK, anti-p-ERK, anti-p38, anti-p-p38, anti-Akt, anti-p-Akt, anti-p-GSK-3β (Cell Signaling), anti-GSK-3β, anti-B-cell lymphoma 2 (Bcl-2) (HuaBio, Hangzhou, China), and anti-bcl-2-like protein 4 (Bax) (Beyotime Biotechnology) antibodies. Subsequently, the membranes were exposed to secondary antibodies for 2 h. The Image Quant LAS 4000mini imaging system (GE Healthcare Bio-Sciences AB, Uppsala, Sweden) was used to quantify the specific proteins. ImageJ software (ImageJ, MD, USA) was used to quantify the autoradiographs.

Statistical analysis

All the results are represented as means ± SD. One-way analysis of variance was used to compare statistical differences among

multiple groups. $P < 0.05$ was considered statistically significant. SPSS 26.0 (SPSS Inc., Chicago, IL, USA) was used to analyze all the data.

RESULTS

β-arrestin2 expression is increased in the liver during AIH development

To elucidate the possible effects of β-arrestin2 in AIH, we established an S-100-induced AIH model. H&E staining revealed inflammatory cell infiltration near the central and portal veins 14 days after modeling. A higher degree of inflammatory cell infiltration and hepatocyte destruction was observed between days 21 and 28 (Fig. 1a). Autoantibodies are a hallmark of AIH, and study has shown that elevated serum ANA levels can be used as an indicator of AIH diagnosis [19]. ELISA revealed that serum ANA levels were higher in the model group than in the control group after 14 days of S-100 treatment; the elevated serum ANA level further increased at 21–28 days (Fig. 1b). In general, liver injury is manifested by elevated ALT and AST activities [20]. We observed that the activities of both ALT and AST were increased in the serum at 21–28 days after S-100 injection (Fig. 1c). To determine β-arrestin2 expression in vivo, we performed Western blotting to detect the time-course expression of β-arrestin2. The results suggest that liver β-arrestin2 expression gradually increased during AIH progression (14, 21, and 28 days) (Fig. 1d). Correlation analysis revealed a positive relationship between liver β-arrestin2 expression in AIH mice and serum ANA levels and ALT and AST activities (Fig. 1e). Taken together, these preliminary findings suggest that β-arrestin2 plays a regulatory role during AIH progression.

β-arrestin2 deficiency ameliorates AIH in mice

To further elucidate the possible effects of β-arrestin2 on AIH, we used *Arrb2* KO mice to establish an S-100-induced AIH model. First, we examined the liver, spleen, and thymus indexes of mice; the results revealed that these indexes were significantly increased after S-100 administration. β-arrestin2 deficiency could reduce these indexes in AIH mice (Fig. S1). H&E staining revealed that the livers of normal mice had a normal lobular structure and cellularity. However, after immunization with S-100, hepatocytes swelled and ruptured, with inflammatory infiltration in the portal area. Nevertheless, the liver of *Arrb2* KO mice exhibited decreased inflammatory cell infiltration, reduced hepatocellular enlargement, and no obvious nuclear lysis after S-100 treatment (Fig. 2a). ELISA revealed that serum ANA levels in AIH mice were significantly increased, whereas those in *Arrb2* KO mice were decreased (Fig. 2b). In addition, we observed that serum AST and ALT activities were markedly elevated in WT model mice but significantly decreased in *Arrb2* KO mice (Fig. 2c).

Studies have reported that AIH pathogenesis is also accompanied by an increase in activated T cells [21, 22]. To elucidate the effects of β-arrestin2 deficiency on activated T cells, we examined the subsets $CD3^+CD4^+$ T cells, $CD3^+CD8^+$ T cells, T helper (Th)17 cells ($CD4^+IL\text{-}17^+$), regulatory T (Treg) cells ($CD4^+CD25^+Foxp3^+$), Th1 cells ($CD4^+IFN\text{-}\gamma^+$), and Th2 cells ($CD4^+IL\text{-}4^+$) in the spleen and liver. Flow cytometry revealed that $CD3^+CD4^+$ T cells, $CD3^+CD8^+$ T cells, Th17 cells, Th1 cells, and Th2 cells were significantly increased and that Treg cells were decreased in the livers of AIH mice. β-arrestin2 deficiency led to a decrease in $CD3^+CD4^+$ T cells, $CD3^+CD8^+$ T cells, Th17 cells, Th1 cells, and Th2 cells and an increase in Treg cells in the livers of AIH mice (Fig. 2d-f). Similar results were obtained for splenic lymphocytes (Fig. S2). Taken together, these findings preliminarily suggest that β-arrestin2 deficiency improves AIH in mice.

β-arrestin2 deficiency reduces hepatocyte apoptosis in AIH

Apoptosis is the predominant pathway for hepatocyte death in the interface hepatitis area, and accelerated apoptosis may be responsible for the severity of liver injury [9, 23]. To determine whether β-arrestin2 affects hepatocyte apoptosis in AIH, we performed the TUNEL assay to assess hepatocyte apoptosis (green fluorescence). We observed that positive cells were increased in AIH mice and that β-arrestin2 deficiency markedly reduced the number of positive cells in AIH mice; this suggests that β-arrestin2 deficiency can significantly reduce hepatocyte apoptosis in the liver tissues of AIH mice (Fig. 3a). In line with the TUNEL assay results, immunofluorescence analysis revealed that the fluorescence intensity of active caspase-3 was enhanced in S-100-induced mouse liver but was decreased in *Arrb2* KO model mouse liver (Fig. 3b). Owing to the high degree of correlation between apoptosis and Bcl-2 and Bax levels [24], we detected their levels using Western blotting and observed that Bax levels were considerably lower but Bcl-2 levels were higher in *Arrb2* KO model mice than in WT model mice (Fig. 3c).

Studies have reported that the activated phosphatidylinositol 3-kinase (PI3K)/Akt signaling pathway can inhibit hepatocyte apoptosis [25]. Recently, a study revealed that β-arrestin2 can regulate Akt signaling [26]. However, it remains unclear whether hepatocyte apoptosis in AIH is related to Akt signaling. Therefore, we investigated the effect of β-arrestin2 deficiency on p-Akt levels in the livers of AIH mice.The results showed that p-Akt levels were higher in *Arrb2* KO model mice than in WT model mice. GSK-3β is an important downstream target of Akt, and Akt can inhibit cell apoptosis by phosphorylating GSK-3β [27]. We also observed that p-GSK-3β levels were significantly higher in the livers of *Arrb2* KO model mice than in those of WT model mice (Fig. 3d). Our results suggest that β-arrestin2 deficiency prevents AIH by activating the Akt/GSK-3β signaling pathway to inhibit hepatocyte apoptosis.

β-arrestin2 deficiency inhibits inflammation and monocyte-derived macrophage infiltration in AIH

The continuous release of inflammatory cytokines can promote hepatocyte apoptosis in AIH [28]. To elucidate the effect of β-arrestin2 deficiency on inflammatory cytokine release, we measured the levels of TNF-α, IL-1β, and IL-6 in the serum and liver. Liver TNF-α, IL-1β, and IL-6 levels were significantly increased in the model mice than in normal mice. However, β-arrestin2 deficiency decreased the levels of these inflammatory cytokines (Fig. 4a). The results obtained for serum were consistent with those obtained for liver tissues (Fig. S3). Taken together, these results suggest that β-arrestin2 deficiency inhibits hepatocyte apoptosis in AIH mice by possibly decreasing the levels of inflammatory cytokines (TNF-α, IL-1β, and IL-6).

Studies have reported the importance of monocyte-derived macrophage infiltration into the liver for AIH pathogenesis and that liver macrophages can produce proapoptotic factors such as TNF-α to induce liver injury [29]. Considering that monocytes and macrophages are the major cells that secrete these factors, the effects of β-arrestin2 deficiency on the infiltration of monocyte-derived macrophages and secretion of TNF-α by macrophages in the livers of AIH mice were examined. F4/80 is a widely used marker for liver macrophages [30]. First, to determine the effect of β-arrestin2 deficiency on the secretion of TNF-α by macrophages in AIH, we used double immunofluorescence staining to detect the expression of F4/80 and TNF-α in mice liver tissues. Single-channel scanning displayed F4/80- and TNF-α-positive signals as green and red fluorescence foci, respectively, with colocalization of these two proteins presented as yellow fluorescence foci. After immunization with S-100, the fluorescence intensities of both F4/80 and TNF-α were decreased in *Arrb2* KO mice than in WT mice. The above result suggests that β-arrestin2 deficiency decreases the coexpression of F4/80 and TNF-α and that β-arrestin2

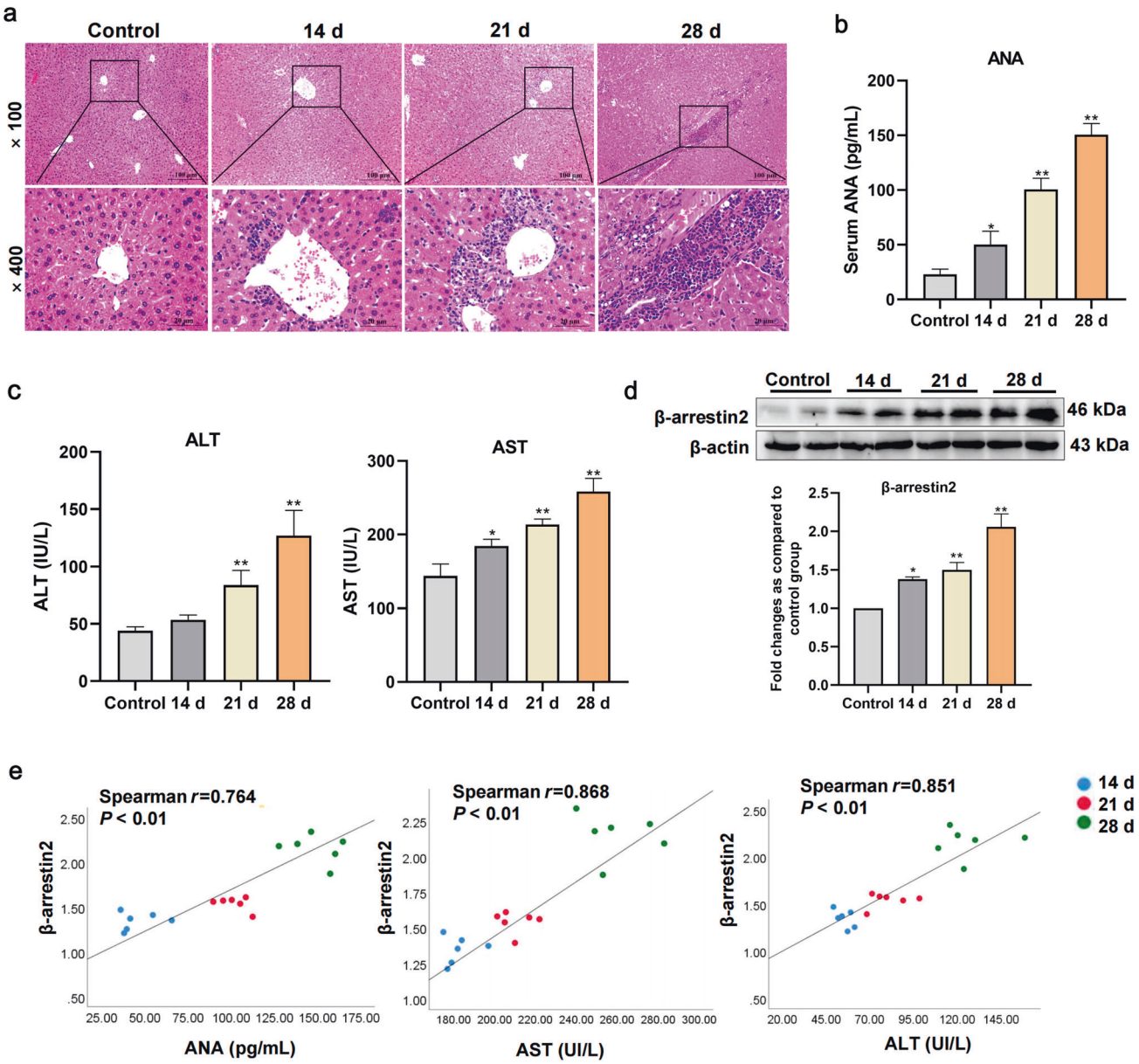

Fig. 1 Expression of β-arrestin2 increased in liver during autoimmune hepatitis (AIH) development. a Representative hematoxylin-eosin staining images of liver tissue in control mice and S-100-treated mice at 14, 21, and 28 days (×100 and ×400 magnifications). **b** Detection of antinuclear antibody (ANA) levels in serum of mice treated with S-100 at different times. **c** Detection of serum alanine aminotransferase (ALT) and aspartate aminotransferase (AST) activities in S-100-treated mice at different times. **d** β-arrestin2 expression in liver tissue of S-100-induced AIH mice at different times was detected using Western blotting. The value of the control group was 1. Representative pictures of the bands are shown. **e** The correlation analyses of β-arrestin2 and serum ANA, ALT, and AST levels during AIH progression. $n = 6$ mice per group. $^{*}P < 0.05$, $^{**}P < 0.01$ compared with the control group.

deficiency can decrease TNF-α secretion by macrophages in AIH (Fig. 4b).

To further investigate whether β-arrestin2 deficiency can inhibit the recruitment of proinflammatory monocyte-derived macrophages, we isolated primary nonparenchymal cells from mice livers for flow cytometry. As described previously, by analyzing CD11b, Ly6C, CD45, and F4/80, we defined four distinct cell subsets [31, 32]. We found that infiltrating monocyte-derived macrophages ($CD45^{+}F4/80^{+}CD11b^{+}$) were significantly increased in S-100-treated WT mice than in normal mice, whereas β-arrestin2 deficiency attenuated this change. However, the number of Kupffer cells (KCs) ($CD45^{+}F4/80^{+}CD11b^{-}$) was not significantly different in the livers of untreated, S-100-treated WT, and *Arrb2* KO mice. Next, we analyzed the phenotype of monocyte-derived macrophages and observed that the ratio of proinflammatory $Ly6C^{high}$ macrophages ($CD45^{+}F4/80^{+}CD11b^{+}Ly6C^{high}$) was increased after S-100 treatment but significantly decreased after β-arrestin2 deficiency. Furthermore, the ratio of restorative $Ly6C^{low}$ macrophages ($CD45^{+}F4/80^{+}CD11b^{+}Ly6C^{low}$) was increased in S-100-treated mice; β-arrestin2 deficiency further increased the ratio of these cells (Fig. 4c). These results suggest that β-arrestin2 deficiency inhibits the recruitment of proinflammatory monocyte-derived macrophages in AIH.

β-arrestin2 plays an important role in monocyte migration

Considering that MCP-1, a chemokine, plays an important role in the recruitment and migration of monocytes [33], we determined MCP-1 expression in liver tissues using Western blotting. We

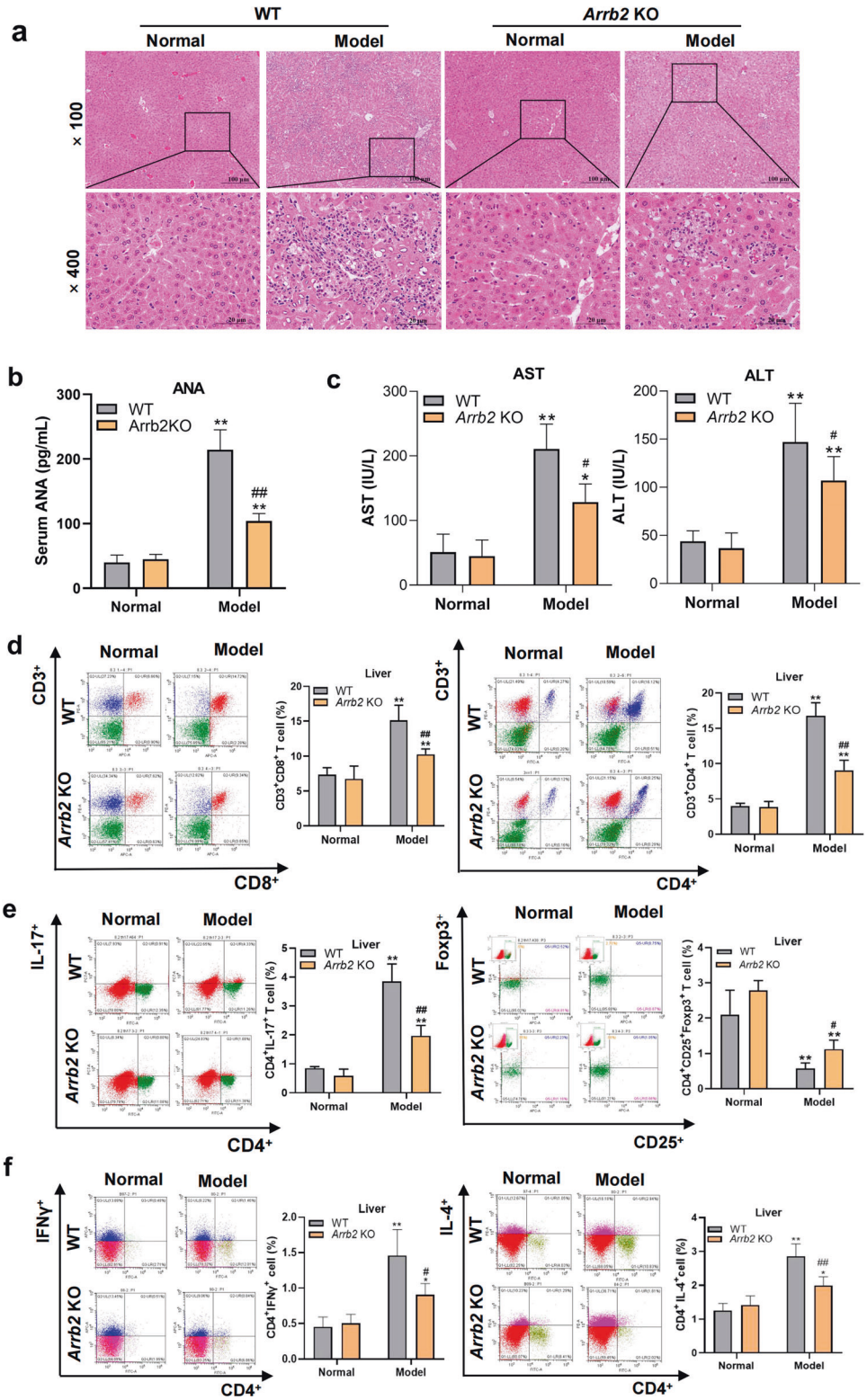

Fig. 2 β-arrestin2 deficiency ameliorates AIH in mice. a Representative liver tissue hematoxylin-eosin staining images from wild-type (WT) and *Arrb2* KO mice treated with S-100 (×100 and ×400 magnifications). **b** Detection of serum levels of ANA in mice treated with S-100. **c** Detection of serum alanine aminotransferase and aspartate aminotransferase activities in mice treated with S-100. **d** The percentages of $CD3^+CD4^+$ T and $CD3^+CD8^+$ T cells in the liver were analyzed. **e** The percentages of Treg ($CD4^+CD25^+Foxp3^+$) and Th17 ($CD4^+IL\text{-}17^+$) cells in the liver were analyzed. **f** The percentages of Th1 ($CD4^+IFN\text{-}\gamma^+$) and Th2 ($CD4^+IL\text{-}4^+$) cells in the liver were analyzed. $n = 6$ mice per group. $^*P < 0.05$, $^{**}P < 0.01$ compared with the normal mice; $^{\#}P < 0.05$, $^{\#\#}P < 0.01$ compared with the WT model mice.

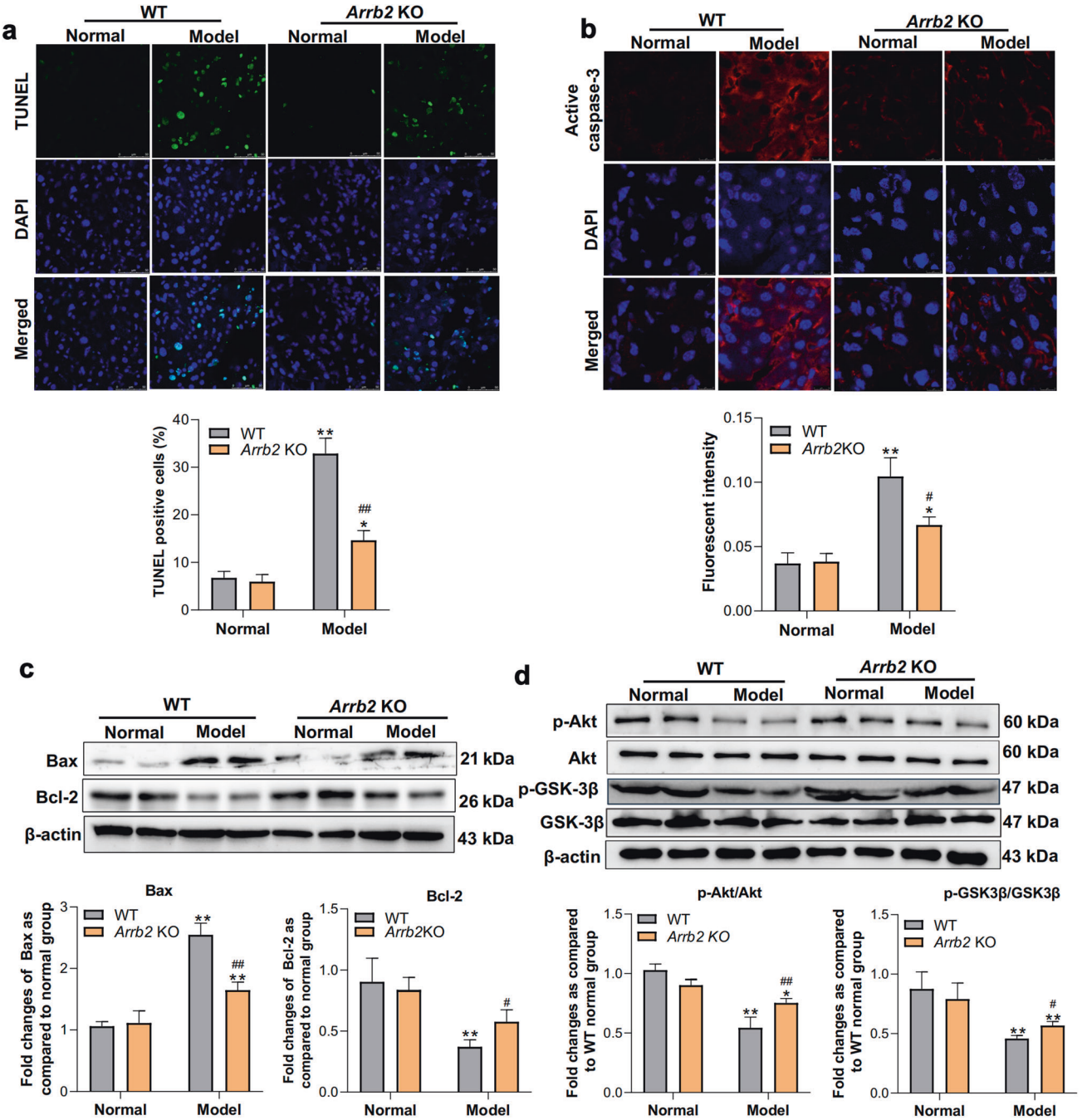

Fig. 3 β-arrestin2 deficiency reduces hepatocyte apoptosis in AIH. a Livers were removed from mice. Apoptotic cells were determined using the terminal deoxynucleotidyl transferase biotin-dUTP nick end labeling staining assay. Representative images in different groups using a fluorescence microscope. **b** The immunofluorescence staining of active caspase-3 in liver tissue was performed using a fluorescence microscope. **c** Western blotting of Bax and Bcl-2 expression, apoptosis-related proteins, from the liver tissue of WT and *Arrb2* KO mice treated with S-100. **d** Liver tissue protein extracts were subjected to immunoblotting for Akt, p-Akt, GSK-3β, and p-GSK-3β. The value of the normal group was visualized as 1. $n = 6$ mice per group. $^{*}P < 0.05$, $^{**}P < 0.01$ compared with the normal group; $^{\#}P < 0.05$, $^{\#\#}P < 0.01$ compared with the WT model group.

observed that MCP-1 expression was increased in the liver of S-100-treated WT mice and that β-arrestin2 level was also increased (Fig. 5a). Thereby, MCP-1-stimulated THP-1 cells were used to study cell migration in vitro.

After treating the cells with different concentrations of MCP-1, we observed that the migration ability of THP-1 cells treated with 10–20 ng/mL MCP-1 was enhanced compared with the control group. Therefore, we used 10 ng/mL MCP-1 to induce cell migration in the subsequent experiments (Fig. S4). To further investigate the effect of β-arrestin2 on monocyte migration, the cells were transfected with the β-arrestin2 overexpression plasmid, followed by Western blotting to confirm successful overexpression (Fig. S5a). We observed that β-arrestin2 overexpression increased the number of migrated MCP-1-stimulated THP-1 cells (Fig. 5b). Next, we blocked β-arrestin2 expression in THP-1 cells using the β-arrestin2 siRNA. Western blotting confirmed that siRNA reduced β-arrestin2 expression in THP-1 cells (Fig. S5b). Additional experiments revealed that the number

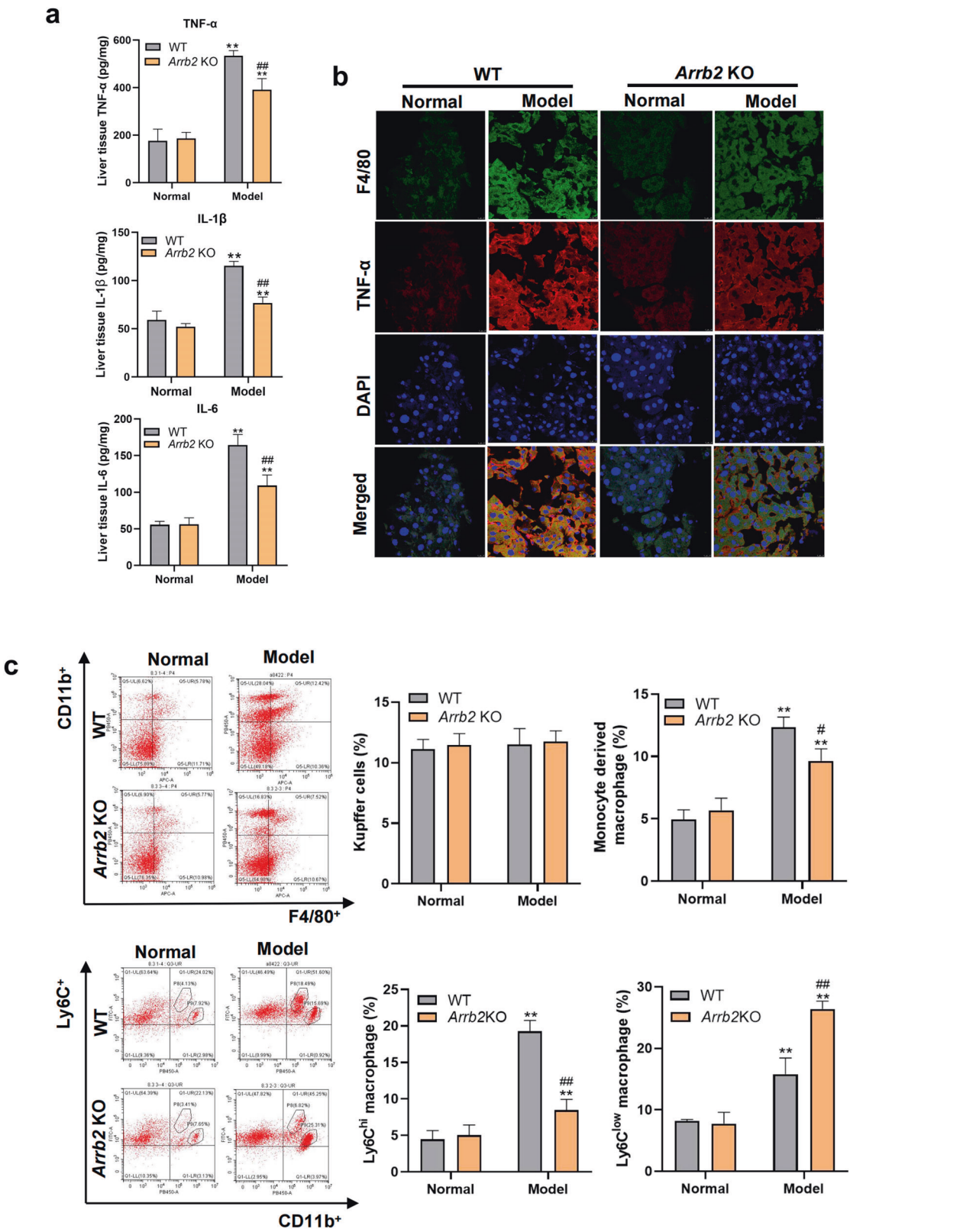

Fig. 4 β-arrestin2 deficiency inhibits inflammation and infiltration of monocyte-derived macrophages in AIH. a Enzyme-linked immunosorbent assay was used to detect the effect of β-arrestin2 deficiency on the production of TNF-α, IL-6, and IL-1β in the liver of AIH mice. **b** Immunofluorescence staining of fixed liver tissue using the murine macrophage-specific monoclonal F4/80 antibodies (green) and TNF-α (red). The nuclei were examined using 4′,6-diamidino-2-phenylindole (blue). **c** CD45, F4/80, CD11b, and Ly6C were used as markers to analyze the changes in three different hepatic macrophage populations in AIH using flow cytometry. A representative staining image is shown. $n = 6$ mice per group. $^{*}P < 0.05$, $^{**}P < 0.01$ compared with the normal mice; $^{\#}P < 0.05$, $^{\#\#}P < 0.01$ compared with the WT model mice.

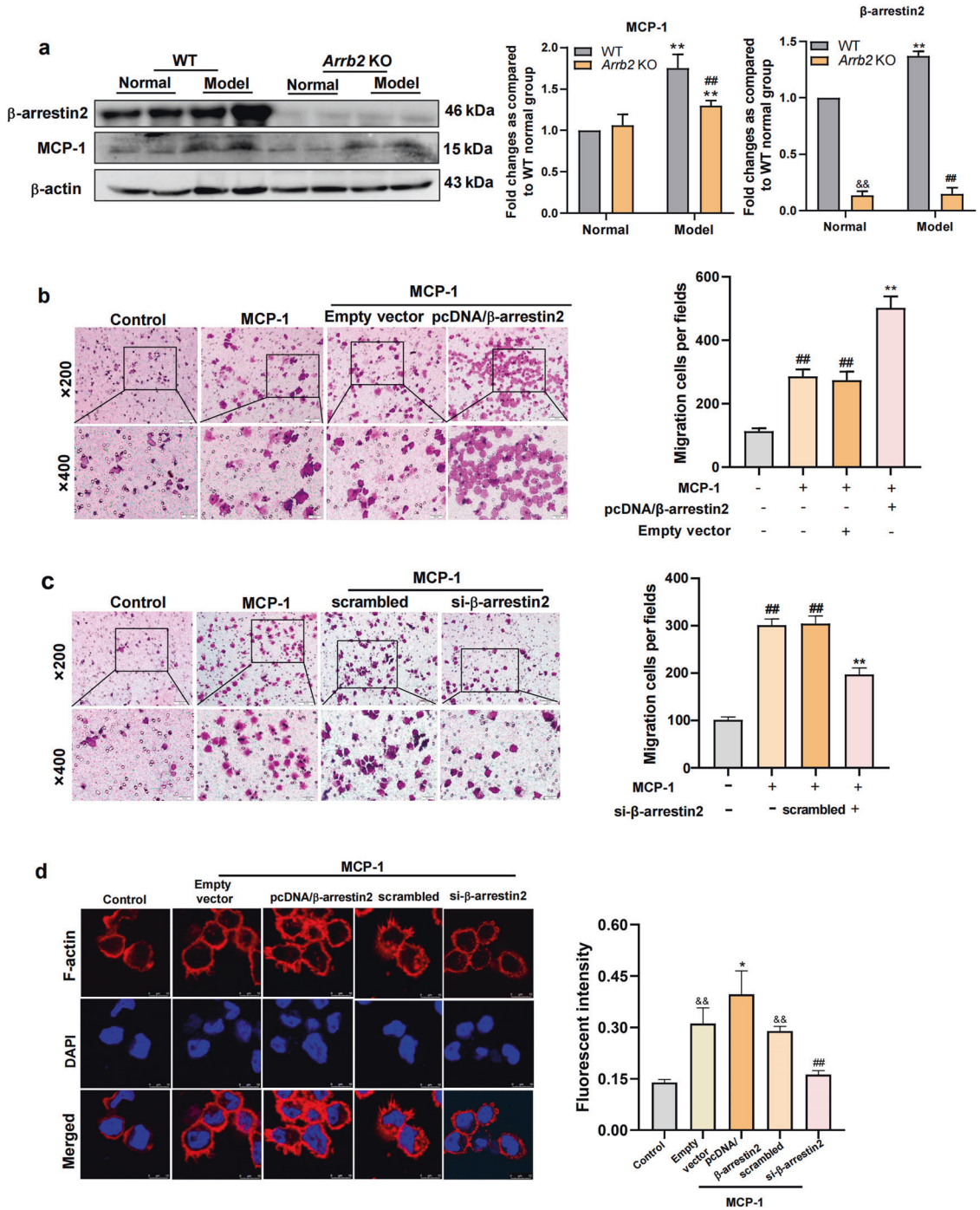

Fig. 5 β-arrestin2 plays a crucial role in THP-1 monocyte migration. a Western blotting of β-arrestin2 and monocyte chemoattractant protein 1 (MCP-1) from liver tissue in AIH. The value of the normal group was visualized as 1. Representative pictures of the bands are shown. $^{**}P < 0.01$ compared with normal mice; $^{\#\#}P < 0.01$ compared with WT model mice. $^{\&\&}P < 0.01$ compared with WT normal mice. **b** Overexpression of β-arrestin2 increased the numbers of migrated THP-1 cells induced by MCP-1. $^{\#\#}P < 0.01$ compared with control group; $^{**}P < 0.01$ compared with empty vector group. **c** β-arrestin2 knockdown decreased the number of migrated THP-1 cells induced by MCP-1. $^{\#\#}P < 0.01$ compared with control group; $^{**}P < 0.01$ compared with the scrambled group. **d** Immunocytochemical staining for F-actin remodeling using TRITC phalloidin (red). The nuclei were examined by 4′,6-diamidino-2-phenylindole (blue). $^{\&\&}P < 0.01$ compared with the control group; $^{*}P < 0.05$ compared with the empty vector group; $^{\#\#}P < 0.01$ compared with the scrambled group.

of migrated THP-1 cells with β-arrestin2 siRNA was significantly decreased compared with untransfected cells stimulated with MCP-1 (Fig. 5c).

Remodeling of the actin cytoskeleton is warranted for monocyte migration [34, 35]. To elucidate the effect of β-arrestin2 on cell cytoskeleton remodeling, immunofluorescence analysis was performed to determine the role of β-arrestin2 in the formation of the F-actin cytoskeleton. F-actin cytoskeleton remodeling was induced upon MCP-1 stimulation, as indicated by the formation of lamellipodia and filopodia. Overexpression of β-arrestin2 is more likely to exhibit F-actin remodeling. β-arrestin2 silencing significantly inhibited the formation of the F-actin cytoskeleton in

MCP-1-stimulated THP-1 cells (Fig. 5d). These findings suggest that β-arrestin2 overexpression promotes monocyte migration and that β-arrestin2 knockdown suppresses monocyte migration.

β-arrestin2 regulates the migration of monocytes via the ERK and p38 MAPK signaling pathways

Studies have revealed that ERK and p38 MAPK pathways participate in various cell migration courses [36, 37]. In this study, we observed that after 2 h of MCP-1 stimulation, the levels of p-ERK and p-38 in THP-1 cells progressively increased and peaked at 30 min (Fig. S6). Further, we confirmed that the inhibition of the activation of ERK and p38 pathways reduced monocyte migration by testing the numbers of migrated THP-1 cells using PD98059 and SB203580 (Fig. 6a). However, it remains to be elucidated whether β-arrestin2 mediates monocyte migration via the ERK or p38 MAPK signaling pathways. We performed Western blotting to observe ERK and p38 MAPK activation after β-arrestin2 overexpression and found that the overexpression of β-arrestin2 could promote ERK and p38 MAPK pathway activation (Fig. 6b). To determine whether the modulation of monocyte migration by β-arrestin2 is related to the abovementioned signaling pathways, THP-1 cells were transfected with a β-arrestin2-overexpressing plasmid in the presence or absence of PD98059 or SB203580. Compared with THP-1 cells transfected only with the β-arrestin2-overexpressing plasmid, the inhibition of the ERK or p38 MAPK reduced the numbers of migrating THP-1 cells after β-arrestin2 overexpression. Therefore, β-arrestin2 overexpression may result in the upregulation of the migration abilities of THP-1 cells by promoting the activation of ERK and p38 MAPK (Fig. 6c). We also evaluated the effects of β-arrestin2 siRNA on the activation of ERK and p38 MAPK signaling in MCP-1-stimulated THP-1 cells. The results revealed that compared with that in MCP-1-stimulated cells, the activation of ERK and p38 MAPK significantly decreased in cells treated with β-arrestin2 siRNA (Fig. 6d). Along with the above findings, β-arrestin2 knockdown reduced THP-1 cell migration; these effects may be achieved via the inhibition of ERK and p38 MAPK activation. Therefore, β-arrestin2 promotes the migration of monocytes via the ERK and p38 MAPK pathways.

β-arrestin2 silencing suppresses the differentiation of monocytes to macrophages via the inhibition of ERK and p38 MAPK pathways

During inflammation or tissue damage, pro-inflammatory mediators attract monocytes migrating to the inflammation site and they differentiate into macrophages for participating in the inflammatory response [38]. PMA-stimulated THP-1 monocytes have been widely used as cell models for the differentiation of monocytes into macrophages [39]. Therefore, we subsequently evaluated whether β-arrestin2 affects the differentiation of monocytes.

We first detected β-arrestin2 expression during the PMA-induced differentiation of THP-1 cells. Western blotting revealed that β-arrestin2 expression gradually increased in a time-dependent manner in PMA-treated THP-1 cells (Fig. 7a). To further understand the effects of β-arrestin2 on PMA-induced monocyte differentiation, we used β-arrestin2 siRNA-transfected THP-1 cells and then treated them with PMA. Pseudopodia growth is a macrophage characteristic for improved adhesion propensity. The pseudopodia growth was found to be reduced in β-arrestin2-silenced cells after PMA stimulation (Fig. S7a). Immunofluorescence staining revealed that the expression of CD68 was lower in THP-1 cells silenced by β-arrestin2 than in the control group (Fig. 7b). Furthermore, the expressions of two monocyte differentiation markers CD68 and CD36 [40, 41] decreased as observed via flow cytometry after β-arrestin2 silencing (Fig. 7c). Altogether, these results indicate that β-arrestin2 knockdown attenuates the differentiation of monocytes. Studies have reported that during the differentiation of monocytes to macrophages, the ERK and p38 MAPK pathways are activated [42]. We also found that ERK and p38 MAPK phosphorylation increased during the process of THP-1 differentiation (Fig. S7b). To clarify whether monocyte differentiation was also regulated by the ERK and p38 MAPK pathways, we used specific inhibitors of ERK or p38 MAPK. These two inhibitors can reduce the expression of CD68 during THP-1 differentiation, similar to β-arrestin2 knockdown (Fig. 7d). Subsequently, we investigated whether β-arrestin2 also influences ERK and p38 MAPK signaling during the differentiation of monocytes into macrophages. Western blotting revealed that β-arrestin2 knockdown attenuated PMA-induced ERK and p38 MAPK phosphorylation (Fig. 7e). Thus, β-arrestin2 plays a critical role in monocyte differentiation by regulating ERK and p38 MAPK signaling pathways.

TNF-α secreted from monocyte-derived macrophages increases hepatocyte apoptosis and the effects of β-arrestin2 on this process

As mentioned, hepatocyte apoptosis in *Arrb2* KO mice was observed to be significantly lower than that in WT mice after S-100 treatment. Furthermore, the levels of TNF-α, a pro-apoptotic cytokine primarily secreted by macrophages, in the liver was significantly reduced. Therefore, we hypothesized that reduced hepatocyte apoptosis is associated with the decreased levels of TNF-α secreted by macrophages, which may be regulated by β-arrestin2. To evaluated the effects of β-arrestin2 on the secretion of TNF-α by monocyte-derived macrophages, we detected the levels of TNF-α in the CM with THP-1 derived macrophages under conditions of β-arrestin2 overexpression or knockdown. ELISA results revealed that β-arrestin2 overexpression could increase TNF-α levels in CM, and β-arrestin2 knockdown reduced the levels of TNF-α (Fig. 7f). To understand whether TNF-α secreted from monocyte-derived macrophages affects hepatocyte apoptosis, we added etanercept (neutralizing antibodies against TNF-α, 5 μg/mL). The results revealed that the apoptosis of L02 cells cultured with CM exhibiting β-arrestin2 overexpression significantly increased, and this elevation was abrogated by etanercept. The apoptosis of L02 cells contrastingly decreased after CM treatment with β-arrestin2 knockdown (Fig. 7g). Therefore, β-arrestin2 was found to increase TNF-α secretion from monocyte-derived macrophages, further inducing hepatocyte apoptosis.

Deletion of β-arrestin2 reduces apoptosis of primary hepatocytes by activating Akt/GSK-3β pathway

Based on the abovementioned findings, β-arrestin2 increased hepatocyte apoptosis by increasing the secretion of TNF-α by monocyte-derived macrophages. Furthermore, it has been reported that β-arrestin2 exhibits a direct regulatory effect on cell apoptosis, such as intestinal epithelial and submandibular gland epithelial cells [43, 44]. However, it remains unclear whether β-arrestin2 directly regulates hepatocyte apoptosis in AIH. To confirm the direct effects of β-arrestin2 on hepatocyte apoptosis in AIH and evaluate the underlying mechanisms, we used TNF-α to stimulate hepatocytes isolated from *Arrb2* KO and WT mice to establish a hepatocyte apoptosis model in vitro. Flow cytometry results revealed that the rate of hepatocyte apoptosis significantly increased under the stimulation of TNF-α at 10 and 20 ng/mL compared with unstimulated cells (Fig. S8a). Western blotting further confirmed these results; treatment with TNF-α at 10 and 20 ng/mL induced an increase in the levels of Bax and β-arrestin2, along with the downregulation of Bcl-2 (Fig. S8b). Therefore, we selected TNF-α at 10 ng/mL as the stimulant for subsequent experiments. To further observe hepatocyte apoptosis after β-arrestin2 deficiency, we subsequently evaluated hepatocyte apoptosis in TNF-α-stimulated *Arrb2* KO mice. The apoptotic rate of TNF-α-stimulated primary hepatocytes was higher than that of untreated hepatocytes in WT mice. However, the apoptotic rate of hepatocytes was significantly reduced in *Arrb2* KO mice under TNF-α stimulation (Fig. 8a). Further experiments revealed that Bax expression increased, whereas the Bcl-2 expression decreased in

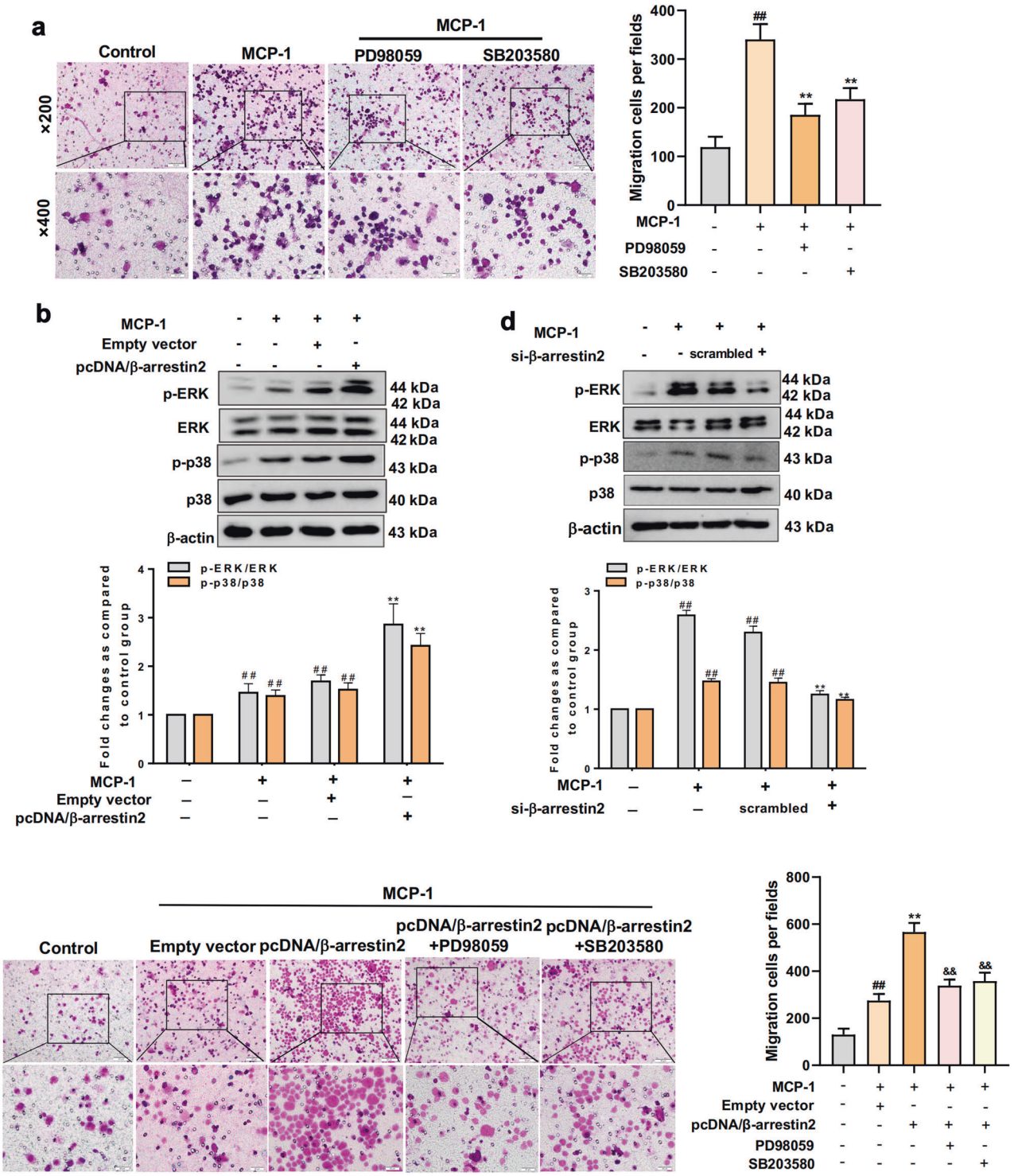

Fig. 6 β-arrestin2 regulates the migration of THP-1 monocytes via ERK and p38 MAPK signaling pathways. a Effects of PD98059 and SB203580 on the migration of THP-1 cells induced by MCP-1 detected using the Transwell assay. $^{\#\#}P < 0.01$ compared with control group, $^{**}P < 0.01$ compared with the MCP-1 group. **b** β-arrestin2 overexpression promoted the activation of ERK and p38 MAPK pathways in THP-1 cells. $^{\#\#}P < 0.01$ compared with control group. $^{**}P < 0.01$ compared with empty vector group. **c** Effects of β-arrestin2 overexpressed plasmid on the migration abilities of THP-1 cells treated with PD98059 or SB203580. $^{\#\#}P < 0.01$ compared with control group; $^{**}P < 0.01$ compared with empty vector group; $^{\&\&}P < 0.01$ compared with the β-arrestin2 overexpression group. **d** Effects of β-arrestin2 siRNA on the activation of ERK and p38 MAPK pathways in MCP-1-stimulated THP-1 cells. $^{\#\#}P < 0.01$ compared with control group; $^{**}P < 0.01$ compared with the scrambled group.

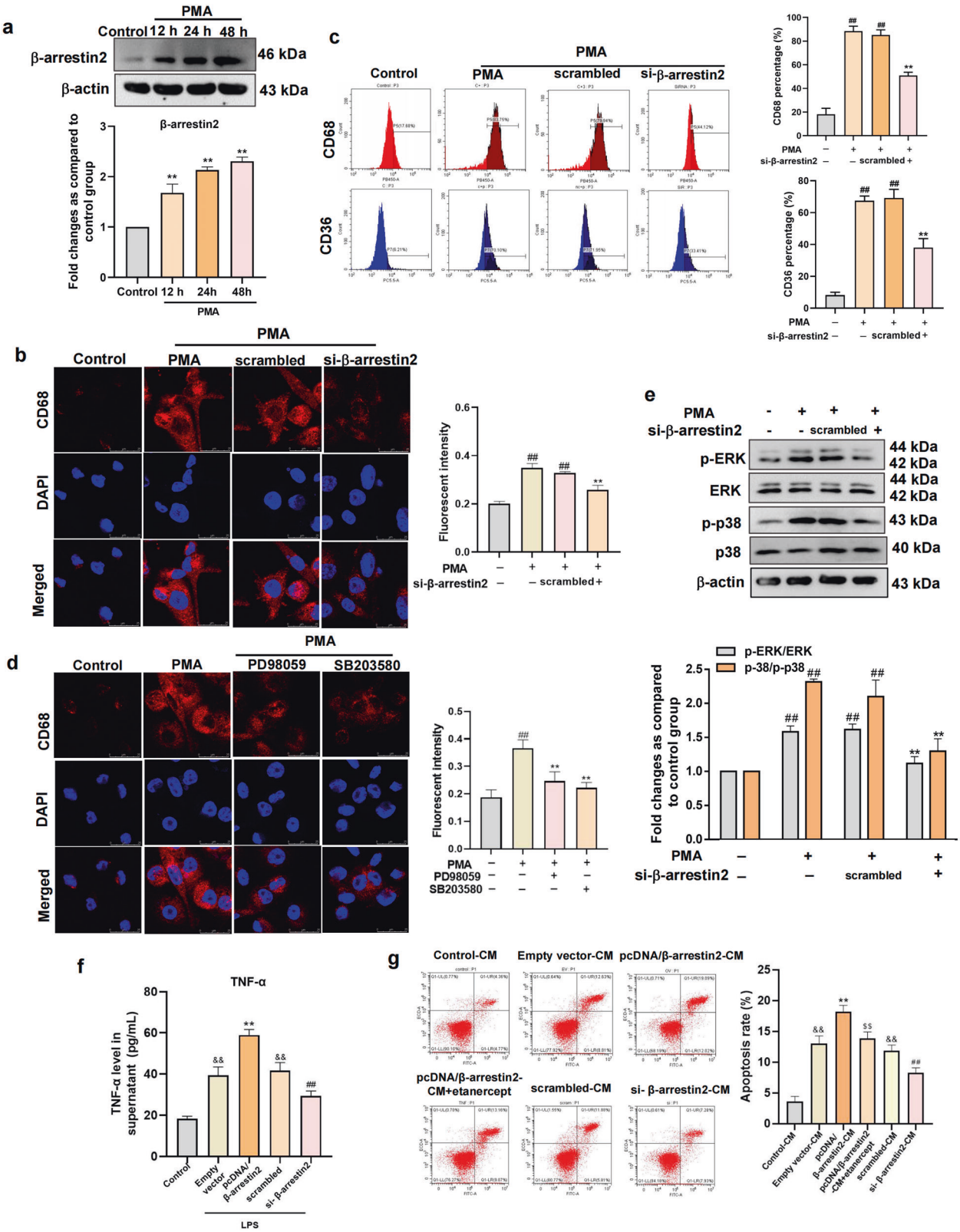

hepatocytes from TNF-α-stimulated WT mice compared with the control group. Deficiency of β-arrestin2 reduces Bax expression and increases Bcl-2 expression under TNF-α stimulation (Fig. 8b). Thus, β-arrestin2 deficiency attenuated TNF-α-mediated primary hepatocyte apoptosis.

To better understand the mechanisms underlying β-arrestin2 involvement in hepatocyte apoptosis, we then detected the p-Akt and p-GSK3β levels of primary hepatocytes. Western blotting revealed that the p-Akt and p-GSK-3β levels in TNF-α-treated hepatocytes were significantly reduced compared with the

Fig. 7 Silencing of β-arrestin2 inhibits differentiation of THP-1 cells to macrophages and reduces hepatocyte apoptosis induced by TNF-α secreted from macrophages. a After treatment with phorbol-12-myristate-13-acetate (PMA) for 12–48 h, β-arrestin2 expression in THP-1 cells was analyzed using Western blotting. $^{**}P < 0.01$ compared with the control group. **b** After transfection with β-arrestin2 siRNA, macrophage surface marker CD68 (red) expression was analyzed using immunofluorescence. The nuclei were examined by 4′,6-diamidino-2-phenylindole (blue). **c** The expressions of CD68 and CD36 in THP-1 cells treated with PMA were detected using flow cytometry after interfering with β-arrestin2 siRNA. $^{\#\#}P < 0.01$ compared with control group; $^{**}P < 0.01$ compared with scrambled group. **d** Immunofluorescence was used to observe the effects of PD98059 or SB203580 on CD68 expression in THP-1 cells stimulated by PMA. $^{\#\#}P < 0.01$ compared with control group; $^{**}P < 0.01$ compared with PMA group. **e** Western blotting revealed the expression of p-ERK and p-p38 in THP-1 cells stimulated with PMA after transfection with β-arrestin2 siRNA. $^{\#\#}P < 0.01$ compared with the control group; $^{**}P < 0.01$ compared with the scrambled group. **f** Effects of β-arrestin2 on TNF-α secretion by monocyte-derived macrophages detected using enzyme-linked immunosorbent assay. $^{\&\&}P < 0.01$ compared with the control group; $^{**}P < 0.01$compared with the empty vector group; $^{\#\#}P < 0.01$ compared with the scrambled group. **g** The apoptosis rates of L02 cells cultured with conditioned media (CM). $^{\&\&}P < 0.01$ compared with the control-CM group; $^{**}P < 0.01$ compared with the empty vector-CM group; $^{\#\#}P < 0.01$ compared with the scrambled-CM group. $^{\$\$}P < 0.01$ compared with the pcDNA-β-arrestin2-CM group.

control group, whereas the levels of p-Akt and p-GSK-3β in TNF-α-treated hepatocytes isolated from *Arrb2* KO mice were increased (Fig. 8c). To further explore whether β-arrestin2 deficiency inhibited hepatocyte apoptosis via Akt signaling pathway activation, we selected LY294002 (Akt inhibitor) to impede this pathway. The results revealed that compared with primary hepatocytes lacking β-arrestin2 without LY294002, LY294002 increased the primary hepatocyte apoptosis in *Arrb2* KO mice (Fig. 8d). These in vitro data are consistent with in vivo results, indicating that β-arrestin2 deficiency may reduce hepatocyte apoptosis via the activation of the Akt/GSK-3β pathway.

DISCUSSION

AIH is a chronic hepatitis and histological condition characterized by the dense infiltration of inflammatory cells in the portal tract [45]. These cells can secrete several pro-inflammatory cytokines, invading the surrounding parenchyma and leading to persistent hepatocyte apoptosis and damage [46]. There are no effective treatments for AIH currently, which seriously threatens human health. Therefore, it is necessary to explore potential therapeutic targets and underlying mechanisms in AIH.

To explore AIH pathogenesis, different AIH models have been developed, including S-100-induced animal models. The pathogenesis of the S-100-induced AIH model is chronic, and the histological changes in the liver are similar to those observed in human AIH [47]. Our current research revealed that β-arrestin2 expression in mice liver significantly increased during S-100-induced AIH development. Further studies revealed that β-arrestin2 expression in the liver was positively correlated with serum ANA, ALT, and AST levels, suggesting that β-arrestin2 is involved in AIH progression.

Some studies have revealed that β-arrestin2 expression is aberrant in several autoimmune diseases. It is highly expressed in the labial gland tissue of patients with Sjogren's syndrome (SS), and β-arrestin2 deficiency reduces epithelial apoptosis and improves the symptoms of the SS mice [44]. The expression of β-arrestin2 in B lymphocytes was apparently increased in collagen-induced arthritis [48]. Furthermore, elevated expression of β-arrestin2 was noted in $CD4^+$ T lymphocytes in asthma model mice [49]. However, the functions of β-arrestin2 in AIH remain to be elucidated. To further investigate the role of β-arrestin2 in AIH, we treated *Arrb2* KO mice with S-100. Hepatic histopathology, serum ANA levels, and liver function were subsequently examined. *Arrb2* KO mice were found to exhibit less inflammatory cell infiltration in the liver and exhibited lower serum ANA levels than WT model mice. Moreover, β-arrestin2 deficiency also reduced the activities of serum ALT and AST, which are indicators of liver function, to certain extent. However, the activities of ALT and AST in *Arrb2* KO model mice did not recover to normal levels in time, which may be because of the fact that S-100-induced AIH is a chronic type of hepatitis and the transaminase activities slowly recovered to normal levels. Thus, β-arrestin2 deficiency could ameliorate S-100-induced AIH.

Increasing evidence suggests that autoreactive T cells are involved in AIH development [50]. A study reported that concanavalin A (Con A)-induced AIH in mice is related to immune and cytokine-mediated autoreactive liver injury, accompanied with the activation of $CD4^+$ and $CD8^+$T cells [51]. Recent studies have also revealed that compared with healthy individuals, the Th1/Th2 and Th17/Treg ratio in the peripheral blood of patients with AIH are imbalanced and positively correlated with disease severity [22]. Increasing evidence has revealed that macrophage infiltration can be influenced by activated $CD4^+$T cells in various autoimmune diseases. For instance, during the development of type 1 diabetes mellitus, several organs are infiltrated by immune cells, and activated $CD4^+$T cells promote the activation and infiltration of macrophages to aggravate the inflammation [52]. $CD4^+$T cells also provoke macrophage infiltration in the eye and lacrimal glands, where they play a functional role in directing the development of autoimmune dry eye in SS [53]. Furthermore, β-arrestin2 participates in regulating the immune system via different pathways. The expression of β-arrestin2 protein has been reported to greatly increase in $CD4^+$ T lymphocytes from a murine asthma model compared with those from WT mice; moreover, β-arrestin2 silencing reduces the accumulation of IL-17 [49]. Our previous study revealed that in mice with liver fibrosis, β-arrestin2 deficiency results in reduced numbers of activated T cells and Th17/Treg ratios [12]. In the current study, β-arrestin2 deficiency decreased activated T cells in the liver and spleen of AIH mice. Thus, β-arrestin2 deficiency may attenuate the inflammation mediated by activated T cells and alleviate S-100-induced AIH.

Considering the crucial role of hepatocyte apoptosis in AIH, we tested hepatocyte apoptosis after β-arrestin2 deficiency. In this model, hepatocyte apoptosis in *Arrb2 KO* mice was observed to be significantly lower than that in WT mice after S-100 treatment. Studies have revealed that prolactin D1 inhibits hepatocyte apoptosis in hepatic IRI by promoting PI3K/Akt pathway activation [54]. Other studies have revealed that decreased levels of phosphorylated GSK3β are correlated with reduced liver injury in BDL mice [55]. β-arrestin2 has been reported to promote hepatocyte apoptosis in mice models of extrahepatic cholestasis by downregulating Akt/GSK3β signaling [55]. However, it remains unclear whether β-arrestin2 deficiency alleviates hepatocyte apoptosis in AIH by regulating the Akt/GSK3β pathway. In this study, p-Akt and p-GSK3β levels were higher in the liver of *Arrb2* KO mice than those in WT mice after S-100 induction. Therefore, β-arrestin2 deficiency inhibits hepatocyte apoptosis by activating the Akt/GSK3β signaling pathway in AIH.

As a potent proapoptotic cytokine, TNF-α induces the dysregulation of apoptosis, which is associated with various autoimmune and liver diseases. Our data revealed that β-arrestin2 deficiency significantly attenuates the increase of TNF-α levels induced by S-100 in the serum and liver. Consistent with the in vivo data, we found that β-arrestin2 could increase the

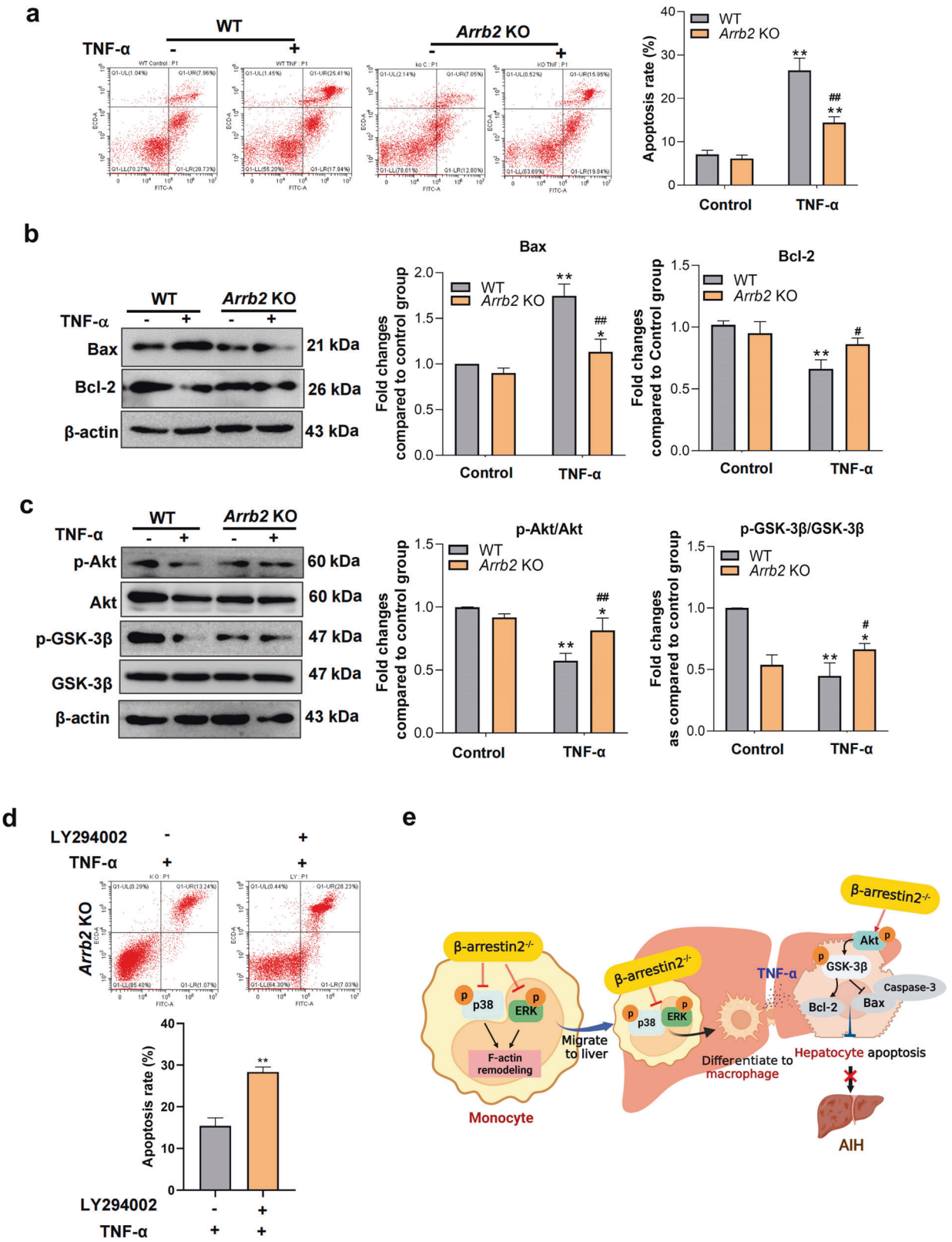

Fig. 8 Deletion of β-arrestin2 reduces apoptosis of primary hepatocytes by activating the Akt/GSK-3β pathway. a Effects of β-arrestin2 deficiency on apoptosis of TNF-α-induced primary hepatocytes were detected using flow cytometry. **b** Western blotting revealed the expression of Bax and Bcl-2 in TNF-α stimulated primary hepatocytes. **c** The protein levels of Akt, GSK-3β, p-Akt, and p-GSK-3β in hepatocytes after TNF-α stimulation were assessed using Western blotting. $^{*}P < 0.05$, $^{**}P < 0.01$ compared with the control group, $^{\#}P < 0.05$, $^{\#\#}P < 0.01$ compared with the TNF-α group. **d** Effect of LY294002 (Akt inhibitor) on apoptosis of hepatocytes from *Arrb2* KO mice. $^{**}P < 0.01$ compared with the TNF-α group. **e** The schematic diagram of the mechanism underlying the regulation of monocyte migration and differentiation by β-arrestin2, further mediating hepatocyte apoptosis in autoimmune hepatitis.

secretion of TNF-α via monocyte-derived macrophages, and TNF-α further induces hepatocyte apoptosis in vitro. Furthermore, β-arrestin2 deficiency also inhibits primary hepatocyte apoptosis induced by TNF-α by directly activating the Akt/GSK3β pathway.

Macrophages are known to be the primary cells that secrete TNF-α. Intrahepatic macrophages consist KCs and monocyte-derived macrophages from peripheral blood [56]. Monocyte-derived macrophages are further divided into pro-inflammatory Ly6C^{high} and restorative Ly6C^{low} macrophages. Ly6C^{high} macrophages aggravate hepatic inflammatory injury by secreting pro-inflammatory cytokines. Ly6C^{low} macrophages exhibit anti-inflammatory effects and promote the repair of tissue injury [6]. In the mouse models of Con A-induced hepatitis, studies have revealed enhanced hepatic recruitment and activation of monocytes/macrophages [57]. Furthermore, immunization against S-100-induced AIH in mice was characterized by marked cellular infiltration and two-thirds of these inflammatory infiltrates were monocytes/macrophages [58]. These results indicate that it is of great significance to study monocyte-derived macrophages in AIH.

Various investigations have revealed that β-arrestin2 is involved in the cellular immune response. A study employing a myocardial infarction mouse model revealed that β-arrestin2 was strongly expressed in infiltrating macrophages, and β-arrestin2 deficiency reduced macrophage infiltration in the infarcted area [59]. Another study revealed that in mice models of allergic asthma, β-arrestin2 deficiency significantly inhibited the infiltration of eosinophils and T lymphocytes into the lungs, reducing the production of inflammatory factors [60]. Because there exists a correlation between the infiltration of monocyte-derived macrophages and AIH, we investigated whether β-arrestin2 deficiency alleviates liver damage in AIH by inhibiting the infiltration of monocyte-derived macrophages. β-arrestin2 deficiency was found to reduce the percentage of pro-inflammatory monocyte-derived macrophages in the liver of AIH mice. Therefore, β-arrestin2 deficiency reduced excessive monocyte recruitment and activation in liver of mice with AIH.

The migration of monocytes is a prerequisite for their recruitment from the blood to the site of injury. Thus, it is necessary to investigate the mechanism underlying monocyte migration. β-arrestin2 serves as a signaling scaffold protein that influences chemotaxis. The chemotaxis of T and B lymphocytes from β-arrestin2-deficient animals were reported to be strikingly impaired [61]. Furthermore, interfering with β-arrestin2 expression in human peripheral blood monocyte-induced macrophages significantly attenuates cellular chemotactic responses [62]. Thus, we explored the effects of β-arrestin2 on monocyte migration. In vitro experiments revealed that β-arrestin2 overexpression increases the number of migrated THP-1 cells, whereas the downregulation of β-arrestin2 decreases the number of migrated THP-1 cells, as detected using Transwell assays. F-actin remodeling is a key element of cell migration [63]. Give that cell migration is accompanied with the dynamic reorganization of the actin cytoskeleton, we labeled F-actin using fluorescent phalloidin staining. In this study, we found that β-arrestin2 overexpression enhanced MCP-1-induced cytoskeletal reorganization in THP-1 cells, as evidenced by the enhanced F-actin stress fiber intensity. In contrast, the cytoskeleton reorganization of THP-1 cells after β-arrestin2 knockdown was observed to be inhibited. Therefore, β-arrestin2 may regulate the migration of monocytes. After monocyte recruitment and their migration, the differentiation of monocytes into macrophages occurs, allowing the monocytes to acquire macrophage characteristics, which is a key step for peripheral monocytes in participating in the inflammatory response [64]. Our in vitro experiments revealed that silencing β-arrestin2 leads to the inhibition of THP-1 cells differentiation into macrophages. Therefore, β-arrestin2 may be an active participant in the differentiation of monocytes to macrophages.

Studies have revealed that β-arrestin2, as a scaffold protein, activates the ERK pathway, mediates the rearrangement of the cellular actin skeleton, and participates in the migration of fibroblasts and tumor cells [65]. Furthermore, β-arrestin2 knockdown blocks chemokine-induced chemotaxis in Th2 cells via the inhibition of the activation of the p38 MAPK pathway [66]. Considering that the phosphorylation of ERK and p38 MAPK also increased during the differentiation of monocytes to macrophages [67], we next determined whether β-arrestin2 promotes the migration and differentiation of monocytes via the ERK and p38 MAPK pathways. Therefore, an overexpressed plasmid or siRNA was transfected into THP-1 cells in vitro, and we observed that β-arrestin2 overexpression promoted the activation of the ERK and p38 MAPK pathways. However, β-arrestin2 knockdown decreased the expression of p-ERK and p-p38 in THP-1 cells. Therefore, β-arrestin2 deficiency may suppress the infiltration of monocyte-derived macrophages in the liver by inhibiting the ERK and p38 MAPK pathways.

In conclusion, we have provided evidence that β-arrestin2 deficiency ameliorates AIH by inhibiting the infiltration of monocyte-derived macrophages in the liver via the inhibition of the migration and differentiation of monocytes. This, meanwhile, reduces inflammatory cytokine-induced hepatocyte apoptosis (Fig. 8e). Targeting β-arrestin2 may be a novel therapeutic approach for preventing AIH and warrants further study.

ACKNOWLEDGEMENTS

This study was supported by grants from the National Natural Science Foundation of China (No. 81770605), the Research Level Improvement Program of Anhui Medical University (No. 2021xkjT016), the Research Fund of Anhui Institute of Translational Medicine (No. 2022zhyx-C07), the Program of Basic and Clinical Collaborative Research (No. 2022sfy014). We acknowledge the help of the staff members of the Institute of Clinical Pharmacology, Anhui Medical University in conducting the study.

AUTHOR CONTRIBUTIONS

WYS, HW and WW contributed to conception and experiment design; TTC, XQL, NL, YPX, YHW, ZYW, MQ and SNZ performed the experiments under the supervision of WYS and WW; TTC and XQL analyzed the data, and drafted the manuscript; WYS, SHZ and HW revised the manuscript. All authors have confirmed the submission of this manuscript.

ADDITIONAL INFORMATION

Supplementary information The online version contains supplementary material available at https://doi.org/10.1038/s41401-023-01103-9.

Competing interests: The authors declare no competing interests.

REFERENCES

1. Beer A, Dienes HP. Autoimmune hepatitis-is histology conclusive? Ann Transl Med. 2021;9:733.
2. Katsumi T, Ueno Y. Epidemiology and surveillance of autoimmune hepatitis in Asia. Liver Int. 2022;42:2015–22.
3. Baeck C, Tacke F. Balance of inflammatory pathways and interplay of immune cells in the liver during homeostasis and injury. EXCLI J. 2014;13:67–81.
4. Longhi MS, Mitry RR, Samyn M, Scalori A, Hussain MJ, Quaglia A, et al. Vigorous activation of monocytes in juvenile autoimmune liver disease escapes the control of regulatory T-cells. Hepatology. 2009;50:130–42.
5. Bartneck M, Fech V, Ehling J, Govaere O, Warzecha KT, Hittatiya K, et al. Histidine-rich glycoprotein promotes macrophage activation and inflammation in chronic liver disease. Hepatology. 2016;63:1310–24.
6. Krenkel O, Tacke F. Liver macrophages in tissue homeostasis and disease. Nat Rev Immunol. 2017;17:306–21.
7. Doherty DG. Immunity, tolerance and autoimmunity in the liver: A comprehensive review. J Autoimmun. 2016;66:60–75.
8. Tu Y, Chen D, Pan T, Chen Z, Xu J, Jin L, et al. Inhibition of miR-431-5p attenuated liver apoptosis through KLF15/p53 signal pathway in S100 induced autoimmune hepatitis mice. Life Sci. 2021;280:119698.
9. Czaja AJ. Targeting apoptosis in autoimmune hepatitis. Dig Dis Sci. 2014;59:2890–904.
10. Latorraca NR, Masureel M, Hollingsworth SA, Heydenreich FM, Suomivuori CM, Brinton C, et al. How GPCR phosphorylation patterns orchestrate arrestin-mediated signaling. Cell. 2020;183:1813–25.

11. Ma TL, Zhou Y, Zhang CY, Gao ZA, Duan JX. The role and mechanism of beta-arrestin2 in signal transduction. Life Sci. 2021;275:119364.
12. Sun WY, Gu YJ, Li XR, Sun JC, Du JJ, Chen JY, et al. β-arrestin2 deficiency protects against hepatic fibrosis in mice and prevents synthesis of extracellular matrix. Cell Death Dis. 2020;11:389.
13. Sun JC, Du JJ, Li XQ, Li N, Wei W, Sun WY. Depletion of β-arrestin2 protects against CCl_4-induced liver injury in mice. Biochem Biophys Res Commun. 2020;522:485–91.
14. Du JJ, Sun JC, Li N, Li XQ, Sun WY, Wei W. beta-Arrestin2 deficiency attenuates oxidative stress in mouse hepatic fibrosis through modulation of NOX4. Acta Pharmacol Sin. 2021;42:1090–100.
15. Sun WY, Sun JC, Li XR, Peng WT, Wei W. Breeding and genotype identification of Arrb2 gene knockout mice. Chin Pharm Bull. 2018;34:878–81.
16. Lohse AW, Manns M, Dienes HP, Meyer zum Büschenfelde KH, Cohen IR. Experimental autoimmune hepatitis: disease induction, time course and T-cell reactivity. Hepatology. 1990;11:24–30.
17. Charni-Natan M, Goldstein I. Protocol for primary mouse hepatocyte isolation. STAR Protoc. 2020;1:100086.
18. Chang YY, Lu CW, Jean WH, Shieh JS, Lin TY. Phorbol myristate acetate induces differentiation of THP-1 cells in a nitric oxide-dependent manner. Nitric Oxide. 2021;109-110:33–41.
19. Galaski J, Weiler-Normann C, Schakat M, Zachou K, Muratori P, et al. Update of the simplified criteria for autoimmune hepatitis: Evaluation of the methodology for immunoserological testing. J Hepatol. 2021;74:312–20.
20. Hwang Y, Kim JC, Tae G. Significantly enhanced recovery of acute liver failure by liver targeted delivery of stem cells via heparin functionalization. Biomaterials. 2019;209:67–78.
21. Ichiki Y, Aoki CA, Bowlus CL, Shimoda S, Ishibashi H, Gershwin ME. T cell immunity in autoimmune hepatitis. Autoimmun Rev. 2005;4:315–21.
22. Liu Y, Yan W, Yuan W, Wang P, Huang D, Luo X, et al. Treg/Th17 imbalance is associated with poor autoimmune hepatitis prognosis. Clin Immunol. 2019;198:79–88.
23. Bai J, Odin JA. Apoptosis and the liver: relation to autoimmunity and related conditions. Autoimmun Rev. 2003;2:36–42.
24. Sharma S, Singh RL, Kakkar P. Modulation of Bax/Bcl-2 and caspases by probiotics during acetaminophen induced apoptosis in primary hepatocytes. Food Chem Toxicol. 2011;49:770–9.
25. Jing ZT, Liu W, Xue CR, Wu SX, Chen WN, Lin XJ, et al. AKT activator SC79 protects hepatocytes from TNF-alpha-mediated apoptosis and alleviates d-Gal/LPS-induced liver injury. Am J Physiol Gastrointest Liver Physiol. 2019;316:387–96.
26. Gu YJ, Sun WY, Zhang S, Wu JJ, Wei W. The emerging roles of beta-arrestins in fibrotic diseases. Acta Pharmacol Sin. 2015;36:1277–87.
27. Zhang X, Jiang W, Zhou AL, Zhao M, Jiang DR. Inhibitory effect of oxymatrine on hepatocyte apoptosis via TLR4/PI3K/Akt/GSK-3beta signaling pathway. World J Gastroenterol. 2017;23:3839–49.
28. Cao L, Quan XB, Zeng WJ, Yang XO, Wang MJ. Mechanism of hepatocyte apoptosis. J Cell Death. 2016;9:19–29.
29. Czaja AJ, Donaldson PT. Genetic susceptibilities for immune expression and liver cell injury in autoimmune hepatitis. Immunol Rev. 2000;174:250–9.
30. Kim SJ, Chang HJ, Volin MV, Umar S, Van Raemdonck K, Chevalier A, et al. Macrophages are the primary effector cells in IL-7-induced arthritis. Cell Mol Immunol. 2020;17:728–40.
31. Ramachandran P, Pellicoro A, Vernon MA, Boulter L, Aucott RL, Ali A, et al. Differential Ly-6C expression identifies the recruited macrophage phenotype, which orchestrates the regression of murine liver fibrosis. Proc Natl Acad Sci USA. 2012;109:3186–95.
32. Zhang M, Liu HL, Huang K, Peng Y, Tao YY, Zhao CQ, et al. Fuzheng Huayu recipe prevented and treated CCl4-induced mice liver fibrosis through regulating polarization and chemotaxis of intrahepatic macrophages via CCL2 and CX3CL1. Evid Based Complement Altern Med. 2020;2020:8591892.
33. Liu Y, Wang W, Zou Z, Fan Q, Hu Z, Feng Z, et al. Monocyte chemoattractant protein 1 released from macrophages induced by hepatitis C virus promotes monocytes migration. Virus Res. 2017;240:190–6.
34. Meconi S, Jacomo V, Boquet P, Raoult D, Mege JL, Capo C. Coxiella burnetii induces reorganization of the actin cytoskeleton in human monocytes. Infect Immun. 1998;66:5527–33.
35. Hu Y, Hu X, Boumsell L, Ivashkiv LB. IFN-gamma and STAT1 arrest monocyte migration and modulate RAC/CDC42 pathways. J Immunol. 2008;180:8057–65.
36. Sun Y, Liu WZ, Liu T, Feng X, Yang N, Zhou HF. Signaling pathway of MAPK/ERK in cell proliferation, differentiation, migration, senescence and apoptosis. J Recept Signal Transduct Res. 2015;35:600–4.
37. Huang C, Jacobson K, Schaller MD. MAP kinases and cell migration. J Cell Sci. 2004;117:4619–28.
38. Jakubzick CV, Randolph GJ, Henson PM. Monocyte differentiation and antigen-presenting functions. Nat Rev Immunol. 2017;17:349–62.
39. Daigneault M, Preston JA, Marriott HM, Whyte MK, Dockrell DH. The identification of markers of macrophage differentiation in PMA-stimulated THP-1 cells and monocyte-derived macrophages. PLoS One. 2010;5:e8668.
40. Chen Y, Yang M, Huang W, Chen W, Zhao Y, Schulte ML, et al. Mitochondrial metabolic reprogramming by CD36 signaling drives macrophage inflammatory responses. Circ Res. 2019;125:1087–102.
41. Chistiakov DA, Killingsworth MC, Myasoedova VA, Orekhov AN, Bobryshev YV. CD68/macrosialin: not just a histochemical marker. Lab Invest. 2017;97:4–13.
42. Bhattacharya A, Ghosh P, Prasad R, Ghosh A, Das K, Roy A, et al. MAP Kinase driven actomyosin rearrangement is a crucial regulator of monocyte to macrophage differentiation. Cell Signal. 2020;73:109691.
43. Zeng LX, Tao J, Liu HL, Tan SW, Yang YD, Peng XJ, et al. β-Arrestin2 encourages inflammation-induced epithelial apoptosis through ER stress/PUMA in colitis. Mucosal Immunol. 2015;8:683–95.
44. Huang L, Liu Q, Zhou T, Zhang J, Tian Q, Zhang Q, et al. Deficiency of beta-arrestin2 alleviates apoptosis through GRP78-ATF6-CHOP signaling pathway in primary Sjogren's syndrome. Int Immunopharmacol. 2021;101:108281.
45. Mieli-Vergani G, Vergani D, Czaja AJ, Manns MP, Krawitt EL, Vierling JM, et al. Autoimmune hepatitis. Nat Rev Dis Prim. 2018;4:18017.
46. Akberova D, Kiassov AP, Abdulganieva D. Serum cytokine levels and their relation to clinical features in patients with autoimmune liver diseases. J Immunol Res. 2017;2017:9829436.
47. Ma L, Zhang LW, Zhuang Y, Ding YB, Chen JP. Exploration the significance of Tfh and related molecules on C57BL/6 mice model of experimental autoimmune hepatitis. J Microbiol Immunol Infect. 2021;54:221–7.
48. Zhou WJ, Wang DD, Tao J, Tai Y, Zhou ZW, Wang Z, et al. Deficiency of beta-arrestin2 exacerbates inflammatory arthritis by facilitating plasma cell formation. Acta Pharmacol Sin. 2021;42:755–66.
49. Liu Y, Wang GY, Liu SK, Yang MY, Ma LB, Li K, et al. β-arrestin2 stimulates interleukin-17 production and expression of $CD4^+$ T lymphocytes in a murine asthma model. Iran J Allergy Asthma Immunol. 2011;10:171–82.
50. Renand A, Cervera-Marzal I, Gil L, Dong C, Garcia A, Kervagoret E, et al. Integrative molecular profiling of autoreactive $CD4^+$ T cells in autoimmune hepatitis. J Hepatol. 2020;73:1379–90.
51. Ye T, Wang T, Yang X, Fan X, Wen M, Shen Y, et al. Comparison of concanavalin a-induced murine autoimmune hepatitis models. Cell Physiol Biochem. 2018;46:1241–51.
52. Li C, Gao Q, Jiang H, Liu C, Du Y, Li L. Changes of macrophage and CD4 T cell in inflammatory response in type 1 diabetic mice. Sci Rep. 2022;12:14929.
53. Zhou D, Chen YT, Chen F, Gallup M, Vijmasi T, Bahrami AF, et al. Critical involvement of macrophage infiltration in the development of Sjögren's syndrome-associated dry eye. Am J Pathol. 2012;181:753–60.
54. Zhang T, Shu HH, Chang L, Ye F, Xu KQ, Huang WQ. Resolvin D1 protects against hepatic ischemia/reperfusion injury in rats. Int Immunopharmacol. 2015;28:322–7.
55. Yin D, Yang X, Li H, Fan H, Zhang X, Feng Y, et al. β-Arrestin 2 promotes hepatocyte apoptosis by inhibiting Akt protein. J Biol Chem. 2016;291:605–12.
56. Xu L, Liu W, Bai F, Xu Y, Liang X, Ma C, et al. Hepatic macrophage as a key player in fatty liver disease. Front Immunol. 2021;12:708978.
57. Almishri W, Shaheen AA, Sharkey KA, Swain MG. The antidepressant mirtazapine inhibits hepatic innate immune networks to attenuate immune-mediated liver injury in mice. Front Immunol. 2019;10:803.
58. Ogawa M, Mori Y, Ueda S, Mori T, Makino Y, Hori J, et al. Protective effects of FUT-175 on acute massive hepatic necrosis induced in mice following endotoxin injection and immunization with liver proteins. J Hepatol. 1993;19:393–400.
59. Watari K, Nakaya M, Nishida M, Kim KM, Kurose H. β-arrestin2 in infiltrated macrophages inhibits excessive inflammation after myocardial infarction. PLoS One. 2013;8:e68351.
60. Walker JK, Fong AM, Lawson BL, Savov JD, Patel DD, Schwartz DA, et al. Beta-arrestin-2 regulates the development of allergic asthma. J Clin Invest. 2003;112:566–74.
61. Fong AM, Premont RT, Richardson RM, Yu YR, Lefkowitz RJ, Patel DD. Defective lymphocyte chemotaxis in beta-arrestin2- and GRK6-deficient mice. Proc Natl Acad Sci USA. 2002;99:7478–83.
62. Cheung R, Malik M, Ravyn V, Tomkowicz B, Ptasznik A, Collman RG. An arrestin-dependent multi-kinase signaling complex mediates MIP-1beta/CCL4 signaling and chemotaxis of primary human macrophages. J Leukoc Biol. 2009;86:833–45.
63. Schaks M, Giannone G, Rottner K. Actin dynamics in cell migration. Essays Biochem. 2019;63:483–95.
64. Shi C, Pamer EG. Monocyte recruitment during infection and inflammation. Nat Rev Immunol. 2011;11:762–74.
65. Ge L, Ly Y, Hollenberg M, DeFea K. A beta-arrestin-dependent scaffold is associated with prolonged MAPK activation in pseudopodia during protease-activated receptor-2-induced chemotaxis. J Biol Chem. 2003;278:34418–426.

66. Lin R, Choi YH, Zidar DA, Walker JKL. Beta-arrestin-2-dependent signaling promotes CCR4-mediated chemotaxis of murine T-helper type 2 cells. Am J Respir Cell Mol Biol. 2018;58:745–55.
67. Tsai CS, Lin YW, Huang CY, Shih CM, Tsai YT, Tsao NW, et al. Thrombomodulin regulates monocye differentiation via PKC delta and ERK1/2 pathway in vitro and in atherosclerotic artery. Sci Rep. 2016;6:38421.